Noise, filters and detection limits*

Xun-Yun Sun[1], Hameraj Singh, Brian Millier, Charles H. Warren, Walter A. Aue*

Department of Chemistry, Dalhousie University, Halifax, Nova Scotia B3H 4J3, Canada

First received 22 March 1994; revised manuscript received 19 August 1994

Abstract

The "noise" of chromatographic baselines has been investigated in regard to the detector, the nature and extent of filtering or smoothing, and the methodologies of qualitative and quantitative assessment: all in order to clarify the role such factors play in the determination and interconversion of some common types of detection limits. This study scrutinizes baselines from the flame photometric detector in single-channel continuous and ten-channel multiplexing versions; it also examines baselines from flame ionization and electron-capture detectors. It makes use of finite impulse response and non-weighted moving-average digital smoothing, as well as three-pole analog filtering.

Baseline fluctuations are quantified by the standard deviation derived from the common root-mean-square (RMS) calculation, or from the less common least-squares Gaussian fit; peak-to-peak noise (N_{p-p}) is estimated by procedures including or excluding presumed outliers. Individual results are expressed as the ratio of N_{p-p} measurement and RMS calculation performed on the *same* data set. A wide variety of such ratios are then assembled from different detectors, filters, and smoothing conditions. They prove conclusively that —contrary to common belief— the conversion factor between the two types of measurements *does* vary: usually between 4 and 10, but occasionally even farther. Consequently, the conversion factor between the corresponding two types of detection limits varies as well.

The N_{p-p}/RMS ratio depends largely on the detector-of-origin, its condition, and the extent to which noise has been filtered. In contrast, the nature and sophistication of the filter hardly matters: either for the N_{p-p}/RMS ratio or for the practical detection limit. This is because the slow undulations characteristic of heavily filtered baselines represent —at least in the detectors we used— dampened fast noise rather than aboriginally slow noise. Corresponding computer simulations, based on amplitudinally random noise smoothed by stationary boxcar or non-weighted moving-average filters, produce results strikingly similar to actual baselines. *Simulated* fast RMS noise correlates, as expected, with the square root (log-log slope = 1/2) of the filter's time constant. The corresponding slopes for *experimental* noise are usually close to 1/2 as well. Most importantly, though, the *simulated* N_{p-p}/RMS ratio varies strongly with the extent of smoothing —thus mimicking and thereby explaining the behavior of the *experimental* ratio.

1. Introduction

Detection limits —in the widest sense of the term— are ubiquitous in the analytical and chromatographic literature, despite the fact that no single technique for their determination has

yet managed to achieve universal acceptance. Indeed, it is not unusual to encounter numbers whose ambiguous derivation or lacking definition make interlaboratory comparison difficult: a situation frequently deplored (e.g. [1]). Even literature from the 1990s often describes detection limits merely as "$S/N = 2$" or "$S/N = 3$", while failing to mention whether N was measured peak-to-peak or root-mean-square (two measurements that differ from one another by far more than 2 differs from 3 —and in the opposite direction to boot). This manuscript is unlikely to change the situation; if anything, it will further complicate it.

There are three general approaches to documenting detection limits in chromatography and beyond. The first is pictorial (and by now rare in the literature, though still our own preference): it displays the recorder trace of a signal small enough, a baseline long enough and noise large enough, to allow evaluation by the analyst. The second and third are numerical: they list the amounts or concentrations or flows at which the signal/noise ratio (S/N) assumes certain quality values, e.g. 2, 3, 10, etc.. Aside from the latter, level-of-confidence parameter, the only difference between the two numerical assessments is the quantification of noise: whether it is measured peak-to-peak (N_{p-p}) or calculated root-mean-square (RMS). Though often poorly defined in practice, so far the matter is well understood.

What is less well understood is the precise relationship of these two numerical assessments. Yet their relationship is of great *practical* value. It holds theoretical interest as well; and it has even affected the promotional efforts of instrument companies. Hence: do these two assessments correlate; can one set of measurements accurately predict the other? If so, what is the *numerical* value of the conversion factor?

Under ideal circumstances of short-term noise and normal (Gaussian) distribution, a reasonable correlation can be established between the theoretically time-dependent N_{p-p} and the theoretically time-independent standard deviation σ of baseline fluctuations in chromatography [2]. In spectroscopy, a widely quoted rule-of-thumb

neglects the effects of sampling time and equates N_{p-p} with five times the RMS noise, where RMS is considered to equal the standard deviation of a Gaussian distribution (e.g. [3,4]). But is chromatographic noise always Gaussian?

One could argue that it really should not matter: all numerical detection limits are single significant digits by definition. A recent book, devoted almost exclusively to detection limits and their meaning, expresses it thus: "One finds, for example, that at least 13 replicates are necessary to obtain s within 50% of the true σ (90% confidence interval)" [5]. If so, the conversion factor between the two detection limits may by its very nature be thought of as similarly vague, i.e. inherently incapable of sharper definition.

But what particular number then to use? The conversion factor of *one*-digit detection limits can legitimately be a *two*-digit number —if justified by its obtainment, of course. The replicates of conversion factors (each from a single set of noise data) are of considerably greater precision than the replicates of noise itself (from several data sets). For instance, one of our earlier studies used 27 noisy baselines, i.e. 27 values of the conversion factor (ratio), in order to determine the latter as the two-digit number $N_{p-p}/\sigma = 5.5 \pm 0.4$; though it did so expressedly "only for our particular measurement techniques and circumstances" [6].

Recently we measured that ratio again on the same detector. However, the detector was now monitored by a radically different (discontinuous, multiplexing) detection system [7], and the new ratio turned out to be significantly smaller than the old one. That was disconcerting. Furthermore, the ratio clearly varied with the extent of data filtering or smoothing.

Note on terms: the verbs "filter" and "smooth" may appear synonymous in this manuscript. However, these terms are not treated as synonyms in the specialized literature [8–12]. There, to "filter" implies an —irreversible and of necessity fast— reduction of noise on data during the acquisition phase; to "smooth" suggests an —often much slower and algorithmically more complex— reduction of noise on already ac-

quired and safely stored data. The same algorithm, if fast enough, can serve as either a "filter" or a "smoother" [8]. In this work, the common three-pole analog filter (resistor–capacitor, RC) is used primarily as a filter but can be employed as a smoother as well; the faster non-weighted moving-average filter (AVG) is designed to function as either a filter or a smoother; and the slower conventional finite-impulse-response filter (FIR) is available as a smoother only.

Back to the main question: why does the N_{p-p}/ RMS ratio vary with conditions? Why should filtering or smoothing change it? Can its change be explained and predicted? To answer these questions, the "nature" of chromatographic noise will have to be further scrutinized. But that brings up a host of new questions. What is the *initial* character (the "unfiltered" distribution) of such noise? Can truly unfiltered noise even be measured? Would it be *source*-dependent, i.e. would it for instance differ among the flame ionization detector (FID), the electron-capture detector (ECD) and the flame photometric detector (FPD)? Would it differ between continuously ("two-dimensional", 2D) and discontinuously ("three-dimensional", 3D) sampled FPD versions? And would all that affect the different approaches used to define detection limits?

Trying to define the barely detectable may literally amount to much ado about (almost) nothing. Yet, in the literature, detection limits are quite frequently discussed and defined [1,2,13–17], even to the extent of a whole book [17]; and they are, by necessity, even more frequently used (and abused).

3. Experimental

All data sets were obtained from chromatographs carrying well-tested and well-proven (though perhaps slightly worn) detectors. The early FPD data came from a Shimadzu GC-4BMP (2D-FPD) model connected to a laboratory-made computer interface; the more recent ones came from the same unit equipped with a 600-rpm wheel carrying a semicircular variable

interference filter, supported by hardware and software for operation as a ten-channel FPD with wavelength as the third dimension (3D-FPD) [7]. The wheel spun at 600 rpm, i.e. at an acquisition time of 5 ms for each 100 ms data point. The FID and the Ni-63 ECD were conventional units (Shimadzu and Tracor, respectively). Detector conditions remained typical of routine operation; they had no obvious bearing on the results of this study.

All raw data flows were routed through a conventional electrometer of RC time constant 0.22 s, with the exception of those coming from the 3D-FPD. The photomultiplier output of the latter was processed by a high-speed amplifier and split into ten 5-ms segments per revolution of the wheel; the data were then assigned to one of three ranges of decadic sensitivity, summed by a gated integrator, converted into digital form, and forwarded to a computer for storage and display [7]. In (our own) "WHEEL" software, two types of low-pass digital filters were available for smoothing operations on the ten-channel data: a non-weighted moving average (hereafter referred to as AVG) with operator-defined window width; and a weighted moving average (a conventional finite-impulse-response filter hereafter referred to as FIR) with operator-defined, fully variable cut-off frequency and the choice of 32, 64 or 128 taps [7]. Half the symmetric table of its weighting coefficients, which follow the Hamming window function, was calculated [18] by

coefficient(m)

$$= \frac{\sin\left[(\text{cut-off frequency}/\text{sampling rate})m\pi\right]}{m\pi}$$
$$\cdot \{0.54 + 0.46 \cos\left[m\pi/(\text{filter taps}/2)\right]\}$$

where $1 < m < (\text{filter taps}/2)$.

The conventional (2D) FPD, the ECD and the FID (the latter via a laboratory-built preamplifier) were monitored on the same Shimadzu GC-4BMPF electrometer, which fed an interface and thence one of our own, two-channel computer programs named "CHROM-8" [19]. This program contains, inter alia, the FIR filter algorithm. It also provides a routine that sorts

baseline fluctuations according to the magnitude of their deviation from the mean (a form of software-based multichannel analyzer), and feeds the resulting array of (raw or smoothed) baseline data to a Dalhousie University undergraduate network program offering least-squares fitting of Gaussian and other types of curves. The enforced Gaussian fit then yields the nominal standard deviation σ_{fit} . (Note that data files can be imported, a pair at a time, from the newer ten-channel WHEEL program into the older two-channel CHROM-8 program —but not the other way around.)

In addition to the smoothing and evaluating functions that are confined to the computer, the raw or treated data flow can be returned from the CHROM-8 program (or from the WHEEL program through the CHROM-8 program) to the analog domain; and it can, via a simple, laboratory-made three-pole filter with a set of time constants, be recorded on a chart (that filter will hereafter be referred to as RC). Raw or smoothed data can also be forwarded directly to a laser printer. And, obviously, the electrometer output can remain completely in the analog domain, i.e. it can provide in the conventional manner (usually via the RC filter) confirmatory baselines or chromatograms on the strip-chart recorder.

The older and newer versions of the laboratory-developed detection limit program[2] differ somewhat in their analytical objective, algorithmic approach, operational convenience, and range of application (though they did not differ, whenever checked, in their results).

The older CHROM-8's "SIGMA" routine [6] employs very heavy digital filtering of the baseline noise (with an operator-adjustable time constant) in order to establish a smooth "zero line" (slightly offset by computational inaccuracies), from which the real baseline fluctuations are measured. The algorithm then uses the

conventional formula for calculating the RMS deviation:

$$RMS = \sqrt{\frac{\sum (x_i - \bar{x}_i)^2}{n}} = \sigma$$

[Note: The definitions use the value, not the ± range of the standard deviation. To use the latter, adjust any derivative equation by an appropriately placed factor of two.]

The newer WHEEL's "DL" program [7] uses a second-order least-squares fit of the baseline (from 50 points selected by the computer at equal intervals on those stretches of the chromatogram that the operator designates as "baseline"). The deviations x_i are then measured from this smooth line. They are used directly (recourse to the mean $\bar{x}_i$ having become superfluous):

$$RMS = \sqrt{\frac{\sum x_i^2}{n}}$$

For this study, n equals 10^3 to 10^4 data points (very roughly 2 to 20 min worth of chromatographic acquisition time).

The DL program proceeds to compute numerical values for the most popular types of detection limits. [Note that these may be associated in the literature with different names —e.g. "detectability", "limit of detection (LOD)", etc. [1,2,13–17]— depending on the analytical circumstance and purpose, the algorithmic formula and the desired level of confidence]. Alluding to disciplinary preferences —but used here solely for ease of reference— we shall denote the algorithmic detection limits based on $S/RMS = 3$ as DL_{spec}, and those based on $S/N_{p-p} = 2$ as DL_{chrom}. Thus,

$$DL_{spec} = 3 \cdot \frac{RMS}{S} \cdot A \text{ (g or mol)}$$

where S is the signal (peak height) and A is the amount injected (presumed to be equal to the amount reaching the detector).

In terms of minimum detectable flow at peak apex (which, for a Gaussian peak of standard

deviation σ_p, is equal to $A/2\sigma_p$), the computer calculates

$$DL_{spec} = 3 \cdot \frac{RMS}{S} \cdot \frac{A}{2\sigma_p} \quad (g/s \text{ or } mol/s)$$

(Note: the computer measures $2\sigma_p$ as the width of the peak, in s, at 60.7% of its height —regardless of its occasionally asymmetric shape.)

To determine the "chromatographic" $S/N_{p-p} = 2$ detection limit on the screen, the operator uses cursors to define the signal S (the peak height) and the peak-to-peak baseline noise N_{p-p}. The latter is available in two versions, depending on whether or not the operator's pattern recognition and judgement is taken into account.

To wit: the first version is "objective" and "inclusive" (i.e. it is independent of the operator and representative of *all* signal excursions, thus including the sharp and strong fluctuations that appear to extend beyond the normal distribution of noise and are hence called "spikes" or "outliers"). We shall name N_{p-p} noise thus measured N_{all}. The second version is "subjective" and "exclusive" (i.e. it allows the operator to define the *core* of the noise, thereby excluding what appear to be spikes). We shall name N_{p-p} noise thus measured N_{core}. Obviously, $N_{all} > N_{core}$ in spiky experimental situations; in simulations (which start with perfect Gaussian distributions), $N_{p-p} = N_{all}$.

The DL calculation, similar to the one above, is then

$$DL_{chrom} = 2 \cdot \frac{N_{p-p}}{S} \cdot A \quad (g \text{ or } mol)$$

and

$$DL_{chrom} = 2 \cdot \frac{N_{p-p}}{S} \cdot \frac{A}{2\sigma_p} \quad (g/s \text{ or } mol/s)$$

(Note: The first number in each equation, i.e. $p = 2$, 3, etc., is the level-of-confidence or probability-related parameter that —for purposes *other* than of this study— can be adjusted to suit analytical objectives or literature definitions.)

Obviously, each of the equations above simply relates the detection limit to the commonly used signal/noise ratio (S/N); with noise being whatever the analyst wants it to be:

$$DL = p \cdot \frac{A}{S/N} \quad (g \text{ or } mol)$$

or

$$DL = \frac{p}{2\sigma_p} \cdot \frac{A}{S/N} \quad (g/s \text{ or } mol/s)$$

(This is both trivial and well-known, as indeed are most of the preceding definitions and relationships. Yet, they needed to be given here again: on one hand to provide a clear record of procedures used; on the other to establish unequivocal terms for discussions to follow. The *new* designations —e.g. N_{all}, N_{core}, σ_{fit}, etc.— are intended for *this* study only. They are not proposed for wider usage: too heavily already is this subject fraught with terms and definitions.)

3. Results and discussion

The prime objective of this study is to address the connection between detection limits that rely on baseline noise as defined by, on one hand, the peak-to-peak (p-p) measurement and by, on the other hand, the root-mean-square (RMS) calculation. This study represents a bottom-up approach (i.e., what does real-life noise look like before and after smoothing?) rather than a top-down enquiry (i.e., what happens mathematically to a temporal array of normal or exponentially modified distributions when exposed to algorithmic filters of different types and varying time constants?) The essential objective of this study thus concerns not the statistics or electronics of the two basic measurements of noise, but the measurements themselves: how does the experienced chromatographer reasonably perform and interconvert them?

This question emphasises the practical. Consequently, a selection of frequently used detectors, filters and evaluation methods is recruited to provide the experimental data. The detectors include the FID, ECD and FPD, plus a variation of the FPD that happened to be available in our

laboratory. The filters include a plain AVG and a sophisticated FIR, as well as a simple three-pole analog RC filter. The evaluation methods include the N_{p-p}-based approach with outliers included (N_{all}) or excluded (N_{core}), and the standard-deviation approach based on the usual calculation (RMS) or the graphical evaluation from an enforced Gaussian fit (σ_{fit}). Not all their possible combinations are explored here; nor would it be reasonable to do so in view of the large number of different detectors and filters that litter the analytical battlefield. However, enough combinations will be investigated to allow general trends to be recognized. The difficulty of recognizing trends will generally increase from comparisons done on a single data file; to comparisons done on several data files from a single set of experiments; to comparisons done on data files from several sets of experiments.

The most important question of this study is whether N_{p-p} and σ-based measurements of baseline noise are linked in any fundamental way. An easy and significant answer to this question can be found in the area of conventional data smoothing.

3.1. Effect of filters on the N_{p-p}/RMS ratio

Fig. 1 provides the answer in one of its simplest and clearest experimental versions. It shows 3D-FPD baseline noise, measured as N_{all}, N_{core} and RMS, as it decreases with the increasing window width of the AVG filter. Clearly, the two types of noise measurement do depend to *different* degrees on the extent of filtering. Their ratio must therefore depend on the extent of filtering as well: the value of N_{all}/RMS changes from approximately 9 at 0.1 s, to 5.7 at 1 s, to (extrapolated) 3.6 at 10 s. And the conversion factor for the two types of detection limits, DL_{chrom} and DL_{spec}, varies accordingly. This may come as a surprise. It is not, however, an experimental singularity: Although Fig. 1 happens to be particularly clear (to the point of being slightly deceptive), it does exemplify a trend evident in almost all of the tested detector–filter combinations.
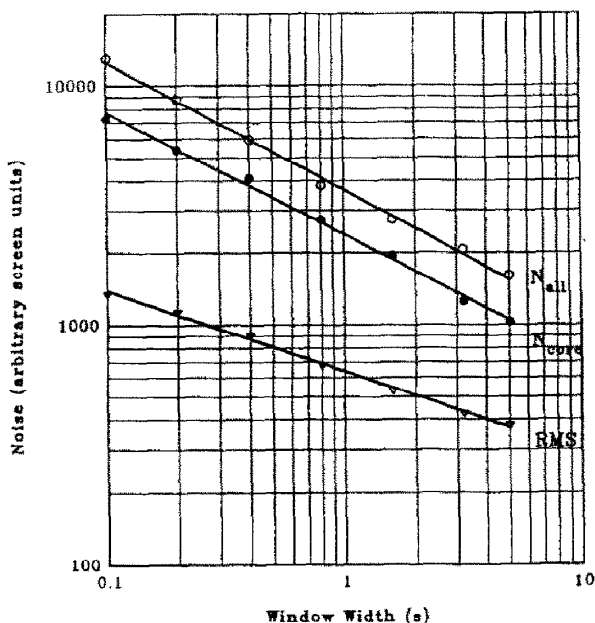
That the N_{all}/RMS ratio should change with

Fig. 1. Variation of three measurements of noise with increasing window width of the AVG filter. Noise: 15 min baseline from segment 2 (ca. 430 to 460 nm) of 3D-FPD [7], H_2 50 ml/min, air 40 ml/min, R-374 photomultiplier tube at -950 V.

the filter time constant did not seem obvious to us at the beginning of this study. We will therefore attempt to make the case for it in general —and deliberately simplistic— terms. In such terms, "noise" can be perceived as deviations of the signal from an imagined smooth ("true") baseline. So, incidentally, can a peak. The analyst's pattern recognition can easily tell the difference between the two. More than just an evaluation of peak width and noise magnitude seems to be involved here: the analyst instantly recognizes the "shapes" of chromatographic peaks. In fact, their characteristically different shapes are still under active investigation [10], mostly by physical chemists. But can chromatographic noise also assume recognizably different shapes?

3.2. Noise "shape"

This question is not quite as silly as it sounds. Recognition of peaks should be easier —mean-

ing the detection limit could be lower— if peaks had shape but noise did not [10,11]. That brings up the question what causes noise, and what modifies it on its way to a determination of the detection limit. Characterization of noise as to its origin, power spectrum, and influence on S/N is particularly well developed in spectrochemical analysis (e.g. [4,20]), and that literature underlies much of the following discussion.

If the noise of, say, an FPD is due to the quantum nature of light ("photon shot noise"), it is random and there should be no shape to it (beyond the shape of the extremely rapid electron avalanches in the photomultiplier tube, of course). If the FPD noise is due to changes in the flame (flicker, fluctuations in column bleed and flow, dust particles, drafts, etc.) it will show these events by their different signatures in different frequency ranges. Such noise will not be random in amplitude; it will be shaped. A similar random/non-random assessment can be made of the complex and still not completely understood processes that translate the random emission of β-rays inside the ECD into the interrelated fluctuations of ion-pair generation and distribution, ion–molecule chemistry, and pulsed charged-particle collection on one hand [21–25]; and the various physical and chemical disturbances known to occur in the ECD on the other. Ditto the chemiionization reaction(s) and sundry associated processes; and the bleeds, leaks, drafts and spikes that produce and/or influence the current of an FID [26].

Thus, ample opportunity exists for initial detector noise to contain recognizable shapes. However, chromatographic detection systems are far too sluggish to display the profiles of the fast "primary" events (FPD photon detection, ECD and FID ion generation and collection). In a typical case, the time constant of the electrometer may be 0.1 s and the full-scale response of the strip-chart recorder 1 s. In addition, analog or digital filters with selectable time constants in the 1–10-s range are often used. Detection limits, in particular, are determined by smoothing the chromatogram as heavily as the concentration profile of the analyte and the conscience of the analyst will allow. The question of "shape" concerns therefore not only the

original but also —and more so— the *filtered* noise.

Different types of filters and smoothing algorithms [9–12,27–29] are often surprisingly similar in the job they do on the noise. This is perhaps best appreciated by considering the job they do on the (much more frequently investigated) analyte peak. The tip of the peak, say its uppermost ten percent, is its most vulnerable part; not surprisingly so since the signal might undergo there a, say, 170° change of direction. Different filters —at least the ones commonly found in chromatographic laboratories— all do adequate noise jobs, but they do clip peaks to different extents.

Let us now imagine that the signal excursions above and below the baseline, which we normally call noise, were a succession of small, sharp peaks. An increase in the severity of data smoothing then means that the sharp tips of these peaks will become round tops, i.e. that they will change their shape from protrusive to pouchy. As this occurs, the peak-to-peak noise will decrease rapidly, the root-mean-square noise will decrease slowly. The ratio of the two noise measurements, $N_{p-p}/$RMS, will therefore change to lower values.

The argument that a shape shift affects the $N_{p-p}/$RMS ratio is further advanced, albeit intuitively, by the geometric metaphor presented in Fig. 2. Its triangular, sinusoidal and hemispherical waveforms are, for simplicity's sake, restricted here to the same single frequency and
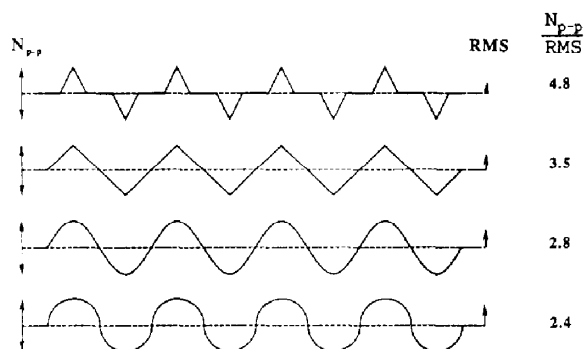

N_{p-p}	RMS	$\dfrac{N_{p-p}}{RMS}$
		4.8
		3.5
		2.8
		2.4

Fig. 2. Geometric figures treated as noise. See text for explanation.

amplitude. {Random distributions of frequency and amplitude could no doubt be called upon to make the resulting waveforms conform more closely to noisy baselines. Even at a single frequency and amplitude, however, the traces already resemble to a remarkable degree what, for instance, IUPAC considers to be noise ([30]; cf. Ref. [31])}

The N_{p-p} values of Fig. 2 are all the same; the RMS values, however, and hence the N_{p-p}/RMS ratios, vary by a factor of two. (They could, of course, vary by much more if the top triangular trace were made a bit spikier). Now imagine analyte peaks of identical height superimposed on these waveforms for purpose of determining their detection limits: all limits based on N_{p-p} would then be the same, while the limits based on RMS would vary by a factor of two. (This raises the question which of the two noise definitions the conscientious analyst could reasonably choose for determining a chromatographic detection limit.)

What Fig. 2 suggests is, in general terms, this: The spikier the excursions of original noise from the "true" baseline (i.e. the larger their ratios of height to width) and the less they are filtered, the higher will be the N_{p-p}/RMS ratio of the noise.

Conversely, the rounder the original noise features, and the more they are filtered, the lower will be the N_{p-p}/RMS ratio. Furthermore, the more severely a particular type of filter crops the tops of baseline excursions, the more it will depress their N_{p-p}/RMS ratio.

3.3. Noise "distribution"

If noise were always normally distributed, there would exist a clear (though sampling-time dependent) statistical correlation between N_{all} and RMS [2]. Conversely, since experiments often show this not to be the case, the distribution cannot always be normal. Consequently we are including σ_{fit} in this study. Fig. 3 shows the particularly poignant example of an FID baseline unsmoothed (though, of course, filtered by the 0.22-s RC time constant of the electrometer). Its spikes suggest that the detector needs cleaning (or perhaps someone came into the room or touched the instrument?). Two spikes appear prominent on the chart-recorded baseline (see insert); these episodes last long enough to enter the distribution as *several* data points. Spikes or not spikes, they exemplify and illustrate a common phenomenon. The standard
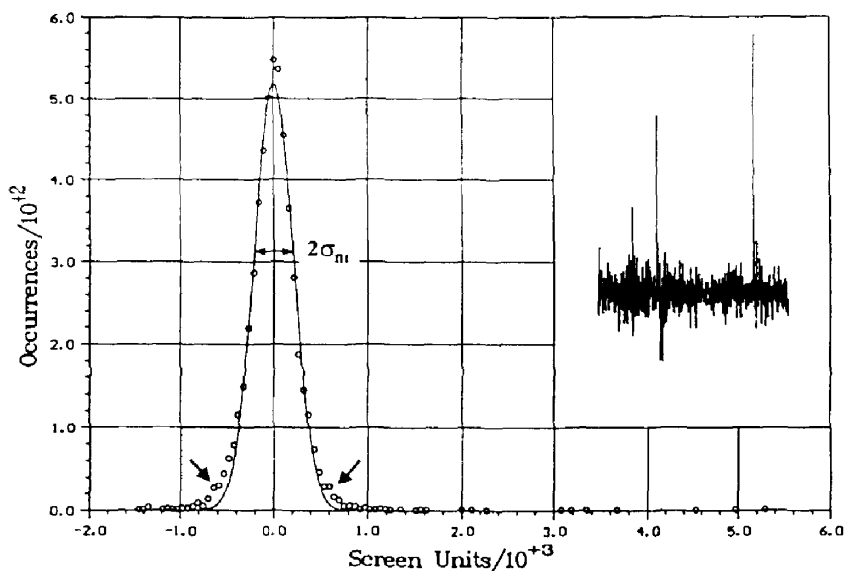

Fig. 3. Example of a baseline with spikes: unfiltered FID noise. Insert: conventional recorder trace.

deviation as measured by RMS is larger here than that measured by σ_{fit}: Even spikes aside, the wings of the distribution (see arrows) are more intense than Gauss allows. Which measurement should then be considered, RMS or σ_{fit}? Which should be considered in other cases of non-Gaussian or superimposed multiple Gaussian distributions?

But these problems are minor —at least in terms of their numerical implications— when compared to the problem of how to measure peak-to-peak noise: N_{all} is about four times as large as N_{core} in Fig. 3, and N_{all}/σ_{fit} is at the ridiculously high value of 30. A strong case could be made here for using the subjective N_{core} rather than the objective N_{all} assessment. (And a strong case could be made for cleaning the detector and smoothing the noise.)

Most detectors are better behaved than the FID of Fig. 3. Normal distributions are often approached. As an example, the top graph of Fig. 4 shows the noise from 22 min of regular FPD operation. Surrounding the solid line of the enforced Gaussian fit are two dashed lines, drawn to demarcate the square-root band at $\pm[(\text{number of occurrences})^{1/2}]$. Asymmetric distributions *not* attributable to spikes can also be encountered. The bottom graph of Fig. 4 shows an example; the solid line again representing the enforced fit, the dashed line indicating what the corresponding author of this manuscript —blissfully unaware of shape and cause— imagined the "true" distribution to look like.

3.4. Noise "speed"

It could be argued that deviations from the Gaussian shape may be due to noise processes of different duration and distribution, which would come sequentially to the fore as smoothing became increasingly effective. That would suggest the presence of weaker and slower (initial) noise components —with time constants within and perhaps beyond the filter range— which became visible only as the stronger and faster components were progressively quelled by the filter.

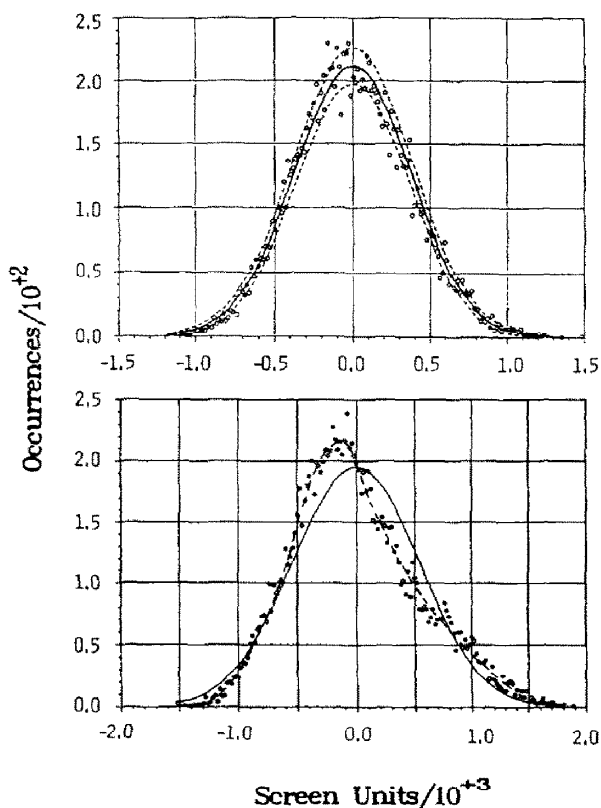However, such does not seem to be the case

Fig. 4. Examples of noise distributions. Upper graph: Gaussian, unfiltered 2D-FPD noise. Solid line: enforced Gaussian; dashed lines: $\pm[(\text{number of occurrences})^{1/2}]$. Lower graph: asymmetric, heavily filtered 3D-FPD noise. Solid line: enforced Gaussian; dashed line: corresponding author's presumption.

here, at least not to any significant extent. If it were, then components slower than the 5-ms segment acquisition time of the 3D-FPD system should appear in two or more wavelength segments (provided they would do so optically) —and they could therefore be annulled or at least significantly decreased by the subtraction of two suitably chosen and scaled segments from one another. (Both our CHROM-8 and WHEEL programs provide the option of subtracting spectrally diverse detector backgrounds or sample matrices [7,19]).

Yet, such an attempt at noise subtraction failed. The noise did not decrease as expected, but instead increased by a factor of ca. $2^{1/2}$ [7]. Furthermore, a similar attempt using continuous,

i.e. electrometer-acquired two-channel data from a conventional FPD, had failed earlier in similar fashion. Thus, at least for these FPD cases, it appears that the relatively slow noise undulations (which figure prominently in heavily filtered baselines) do *not* originate as slow noise in the detector (e.g. as flame or flow flicker). Rather, they must owe their existence to fast noise being converted into slow.

3.5. Sundry detectors, sundry filters

We return to evaluating further combinations of detectors and filters. Table 1 presents a selection of four typical noise sources, all treated by the *same* filter. This selection includes conventional electron-capture and flame ionization detectors, the FPD in the intermittently sampled 3D version, and a conventional photomultiplier tube's dark current. Other systems behave similar. Note that the results of Table 1, representing noise or noise-ratio measurements by various definitions, may be compared only with due caution. They carry, at best, two significant digits —as, indeed, one expects them to. The important data —in terms of addressing various definitions of detection limits— are, of course, the ratios as given in the last four columns. (The

Table 1
FIR smoothing of noise from different sources

FIR cut-off[a]	N_{all}	N_{core}	RMS	σ_{fit}	N_{all}/RMS	N_{all}/σ_{fit}	N_{core}/RMS	N_{core}/σ_{fit}
^{63}Ni-ECD, d.c. mode, 5 min								
None	3 280	2 700	533	557	6.2	5.9	5.1	4.8
2	3 060	2 500	514	520	6.0	5.9	4.9	4.8
1	2 630	2 200	464	472	5.7	5.6	4.7	4.7
0.5	2 090	1 760	367	358	5.7	5.8	4.8	4.9
0.2	1 060	837	210	238	5.0	4.5	4.0	3.5
0.1	556	500	116	133	4.8	4.2	4.3	3.8
FID, 10 min								
None	14 300	7 130	1 100	875	13.0	16.3	6.5	8.1
2	12 800	5 730	984	792	13.0	16.2	5.8	7.2
1	7 720	4 400	758	628	10.2	12.3	5.8	7.0
0.5	4 630	2 800	482	426	9.6	10.9	5.8	6.6
0.2	1 550	1 100	224	216	6.9	7.2	4.9	5.1
0.1	711	617	122	122	5.8	5.8	5.1	5.1
3D-FPD, segment 4 (ca. 490–520 nm), 10 min								
None	16 900	10 100	2 580	2 490	6.6	6.8	3.9	4.1
2	7 860	4 330	1 160	1 150	6.8	6.8	3.7	3.8
1	5 060	2 710	780	774	6.5	6.5	3.5	3.5
0.5	3 310	1 800	522	530	6.3	6.2	3.4	3.4
0.2	1 660	930	276	253	6.0	6.6	3.4	3.7
0.1	899	520	159	142	5.7	6.3	3.3	3.7
Dark current, R-374 photomultiplier tube, −760 V, 5 min								
None	3 100	2 000	380	390	8.2	7.9	5.3	5.1
2	2 800	1 870	360	380	7.8	7.4	5.2	4.9
1	1 800	1 500	290	290	6.2	6.2	5.2	5.2
0.5	1 200	870	180	200	6.7	6.0	4.8	4.4
0.2	440	380	84	88	5.2	5.0	4.5	4.3
0.1	230	210	46	50	5.0	4.6	4.6	4.2

[a] In Hz, nominal.

first four columns of plain noise measurements have been included for purpose of complete documentation only. These data, coming as they do from different detectors, conditions, amplifiers, attenuations, etc., are of necessity given in arbitrary units and are hence comparable only within a particular set, not across the whole table.)

Table 1 suggests that different noise sources do produce *different* types of noise to start with. The highest and the lowest ratios in the "non-filtered" mode are about a factor of two apart. (The FID used here is somewhat cleaner than the one that produced Fig. 3.) The assumption of *different* types of noise is also supported by different distributions. In a perfectly Gaussian distribution, RMS and σ_{fit} are the same; and so are the ratios N_{all}/RMS and N_{all}/σ_{fit}. Examination of Table 1 shows, however, that the two measurements differ to a small but significant extent. Now, RMS is larger in the FID (as expected from Fig. 3) and the 3D-FPD; while σ_{fit} is larger in the ECD and the covered photomultiplier tube. These relationships hold (with minor exceptions) *throughout* the monitored smoothing ranges. Yet the differences between RMS and σ_{fit} are relatively small.

Perhaps the most striking trend apparent in Table 1 is that all the ratios decline (again with minor exceptions) as the extent of FIR smoothing increases. This parallels the relationships obtained with the AVG filter as portrayed in Fig. 1. Fig. 1 is, however, somewhat limited: the AVG filter is restricted to a window width of 50 data points, i.e. 5 s [7]. In contrast, the time constant of the FIR smoother is unrestricted. Fig. 5 presents therefore a close-up look at the ratios in two detectors —conventional FPD on top, FID on the bottom— over an FIR filter range that extends to longer time constants and includes more data points. The found dependence is illustrated by solid least-square linear regression lines. Note that, given the kind of subject and the type of plot, the data points are *expected* to show considerable scatter. Note also that these baselines —in contrast to those of Fig. 1— were obtained from an electrometer of RC time constant 0.22 s: consequently it would have
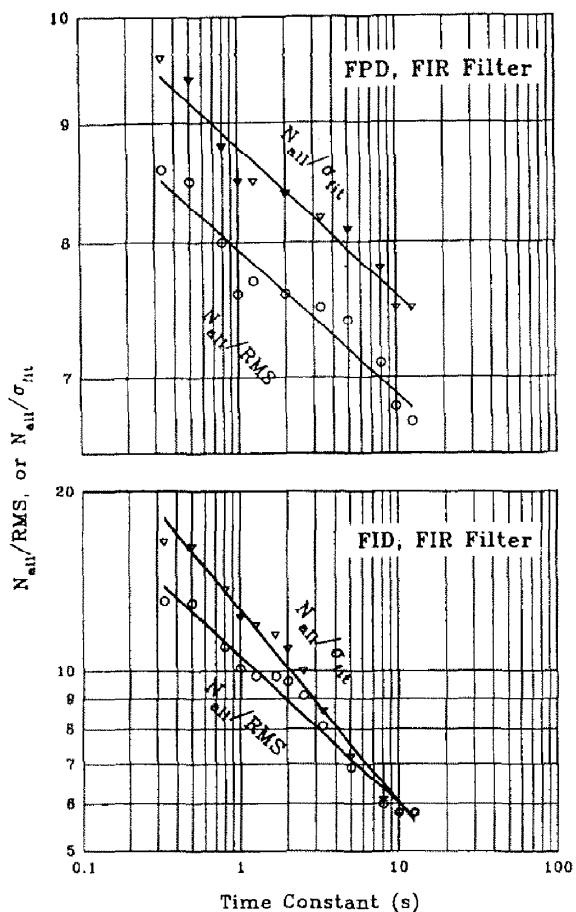

Fig. 5. Variation of N_{all}/RMS and N_{all}/σ_{fit} ratios with FIR smoothing of FPD and FID noise. The nominal time constant is the reciprocal FIR "cut-off frequency" (see Experimental). The solid lines are linear least-squares regression fits. Upper graph: 12 min of conventional FPD noise. Non-filtered ratios (straight from RC time constant 0.22 s electrometer): 9.7 and 8.8. Lower graph: 10 min conventional FID noise. Non-filtered ratios: 16 and 13.

made little sense to measure data points below that value.

Fig. 5 confirms that the N_{all}/RMS and N_{all}/σ_{fit} ratios decrease as the influence of the smoothing algorithm increases. The N_{core}/RMS and N_{core}/σ_{fit} ratios are not shown here; they display similar though somewhat less dramatic behaviour. So far the ratios behave as expected. However, so far we have considered only numerical, not visual behaviour —and the interrelated topics of noise, filters and detection limits

may contain significant perceptual components. Better expressed: "anyone who tries to analyse a time series without plotting it first is asking for trouble" [32].

3.6. Plotting experimental noise

One potential troublespot in this study is the N_{core} definition. We have no better way of defining what the first author perceived to be "core" noise than by displaying the results of his efforts on a 3D-FPD sample plot. In Fig. 6, the subjective N_{core} measurement is shown on the right, the objective N_{all} measurement on the left; for AVG window widths ranging from 0.1 (unfiltered) to 5 s.

(Note: It would have been easy for us to replace the analyst-assessed limits of N_{core} by a computer-calculated test for outliers —thereby changing N_{core} into a seemingly "objective" measurement. Indeed, such may be a reasonable action to propose if —and that is a psychologically insurmountable if— the scientific community were likely to agree on a binding set of rules for determining detection limits. But, in the context of this exploratory study, it would make little sense to introduce outlier tests for despiking baselines. Furthermore, we would not want to add to chromatographic practice yet another hidden algorithm whose precise effect on peak and noise is difficult to evaluate.

Beyond documenting the first author's holistic, subliminal perception (cf. [33]) in defining N_{core}, and beyond providing the visual record of a sample data file, Fig. 6 offers still further material for discussion. For instance: after about 1 min into the record, the top trace shows two strong, positive excursions. These persist in two more traces below, then subside. In contrast, the strongest positive excursion of the bottom trace occurs at about 4.25 min. Its presence can be followed up to the top trace, but just barely. So why do traces of different time constants emphasize different episodes?

The human eye is attracted to the highest amplitude of an individual excursion (the "record performance"); and so, of course, is the measurement of N_{all}. Filters, on the other hand,
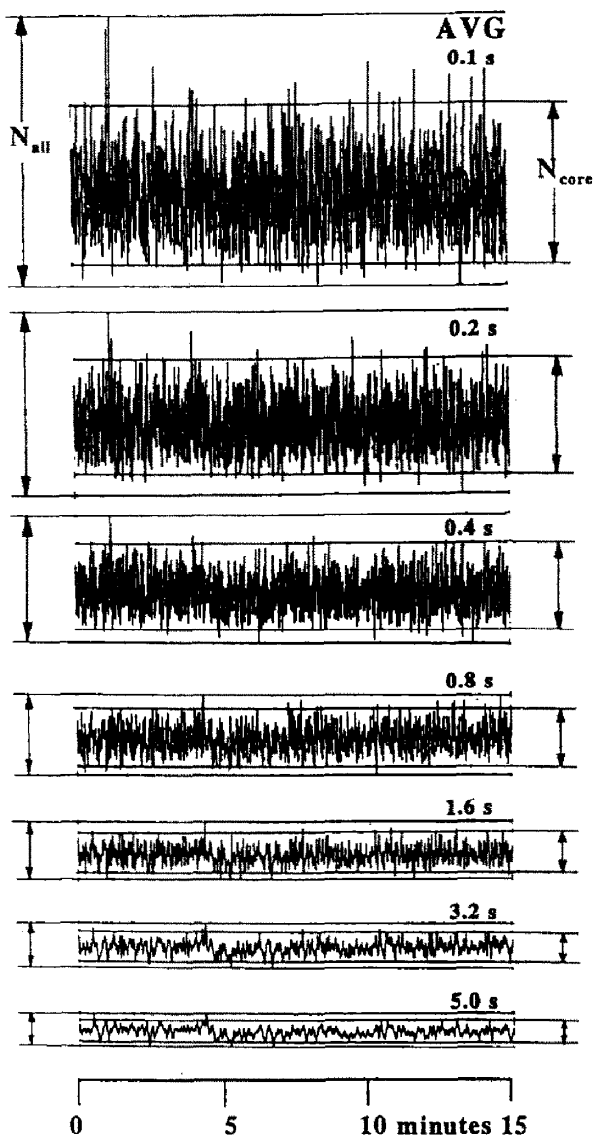

Fig. 6. Traces of AVG-smoothed 3D-FPD noise, comparing N_{all} measurements and N_{core} estimates. Laser printer.

take a broader view: they simply redistribute net total energy. A strong but lone excursion, dominant under light smoothing, might lose that dominance under heavy smoothing to a few weaker but closely positioned, equidirectional and hence mutually reinforcing excursions. (This effect can be observed in many human activities, including scientific evaluation. In a manner of speaking, even N_{p-p} and RMS differ in the way they see noise as individual and collective phe-

nomena, respectively.) Different groups of noise excursions thus appear in time windows of different width; and recognizing particular noise episodes —whether original or derivative in nature— depends on choosing the correct time domain. For the present system such an interpretation implies that originally fast noise is being converted into visually slow noise by the filter. This conclusion is supported by our earlier-described failure to eliminate what appeared to be slow noise from 2D- and 3D-FPD chromatograms [7]; it will also be supported by later simulations resulting in square-root relationships.

To be sure, this only means that truly slow system noise did not exist to any significant extent in the baselines here considered; in many other chromatographic and spectroscopic systems it may well be present (e.g. as so-called "$1/f$" or "pink" noise [4]). If the latter is the case, then the filter may not just convert fast noise into seemingly slow noise, but it may also remove fast noise from genuinely slow noise. In Fig. 6, however, there is little or no evidence of that.

Fig. 6 can be analyzed by more than *visual* perception. Its raw data are the same as those of the earlier Fig. 1 —and combined these two figures raise several interesting and, more importantly, easily answered questions. In Fig. 1, the relationship of noise to window width (filter time constant) appears linear. Furthermore —although surprisingly and perhaps spuriously more so for N_{all} and N_{core} than for RMS— the slope is close to one half, suggesting a classical square-root dependence based on the randomness of noise. If *all* initial noise were indeed fast and normally distributed, would that translate into an amplitudinal square-root relationship of noise with the filter's time constant? Would *both* N_{all} and RMS obey it —i.e. would they perhaps become parallel and would the N_{all}/RMS ratio therefore become constant? The question is not trivial: such parallelism, if it were to occur, would provide support —of a theoretical if not of a practical nature— for proposing a *single* rule-of-thumb factor that could then be used, generally and legitimately, to interconvert the two types

of measurements. For an answer to these questions, a purely Gaussian noise file is needed.

3.7. Plotting simulated noise

Random noise can be easily simulated. For expediency's sake we take a shortcut here and start from a preformed Gaussian distribution of noise *amplitudes* (despite the fact that most if not all of the random elements in initial noise are in the *time* domain). What is presumed random and dominant in initial noise are, of course, the *temporal intervals*: between photomultiplier tube electrons being ejected by photons in the FPD, between β's being emitted in the ECD, between charged particles being formed and collected in the FID. Seen through larger filter windows, short intervals between these primary events appear as positive, long intervals as negative amplitudinal excursions.

Note that, for purpose of noise calculations, the *initial* FID events can be assumed to have the same amplitude, i.e. that of a unit charge; and the photomultiplier tube electron avalanches can be assumed to be of similar strength (at least those avalanches set off by photons from the FPD flame). In contrast, the ECD's ion-pair yield of individual β-rays varies —in a predictable, inherent manner due to the comcomitant loss of neutrinos; in a much less predictable, condition-dependent manner due to the particulars of isotope plating, cell dimensions, foil contamination and β backscattering from nearby surfaces [34,35].

For the purpose at hand, Gaussian noise is generated either by a commercial program (Sigmaplot), or by blindly drawing marked paper squares (a tessellated Gaussian) out of a well-mixed bowl. (Within the expected variation, the results are the same. Later and longer simulations are therefore based on Sigmaplot inputs only.) Two types of averaging algorithms are used: a stationary boxcar and a non-weighted moving window [8—12]. The boxcar mimics the action of the gated integrator [7] in the 3D-FPD's fast acquisition circuit (although the length of the former is variable while that of the latter is fixed at 5 ms). The moving window

parallels the action of the AVG filter. The N_{all} and RMS values can be easily calculated, once the compromised start and end pieces (of half the boxcar length or window width) are removed.

The left side of Fig. 7 shows the visual effects of the AVG filter. (The boxcar traces look similar, but are computed only to a boxcar "length" —or "load"— of 64 initial data points.) Both types of simulated baseline look very much like the real one shown in Fig. 6; except that, there, some spikes are present and the window can open to only 50 data points. The earlier-discussed waxing and waning of particular experimental noise episodes across adjacent windows of different width can be observed in the simulated traces of Fig. 7 as well; thus adding weight to the adopted interpretation.

The numerical $N_{p\text{-}p}$ ($= N_{all}$) and RMS noise variation with window width and boxcar length is shown in Fig. 8. The points are averages of five replicates; from different random inputs, of course, and replete with standard-deviation error
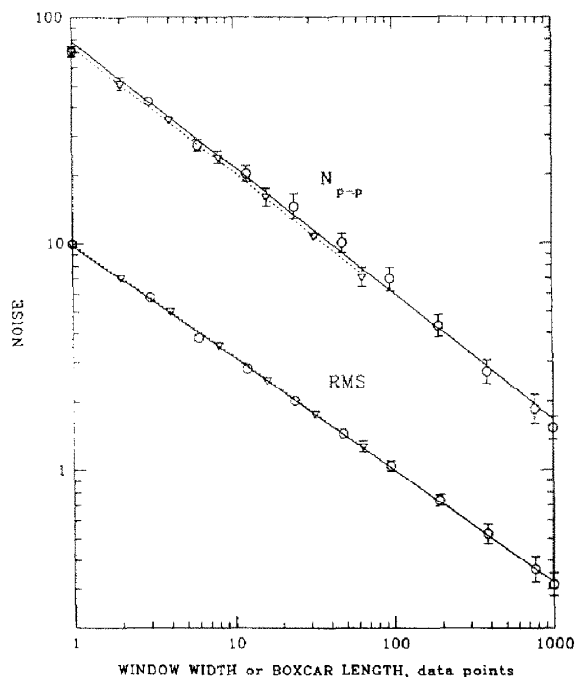

Fig. 8. Measurements on simulated single-frequency Gaussian noise, smoothed by boxcar (∇) and AVG ($\bigcirc$) filters. Data points are averages of five independent sets (one AVG set is shown on the left side of Fig. 7).

bars on the least-squares linear regression lines. As expected, the two filters behave alike. Also as expected: it is the RMS line now that shows the square-root slope. The $N_{p\text{-}p}$/RMS ratio declines, over three orders of time variation, from roughly 8 to roughly 5. Compared to the experimental Fig. 1, this decline is somewhat less steep.

Far more important in the present context, however, is the fact that the "theoretical" $N_{p\text{-}p}$/RMS ratio of initially Gaussian noise is filter-width *dependent*, just as is the experimental ratio. In other words, in the absence of additional information about a particular system, the analyst can *not* correlate its two noise measurements $N_{p\text{-}p}$ and RMS —and, more importantly, its corresponding detection limits DL_{chrom} and DL_{spec}— by simply assuming the initial noise to be Gaussian. Even if that primary assumption were correct, it would not justify the use of a constant factor for the interconversion of $N_{p\text{-}p}$ and RMS. Note also that this particular simula-
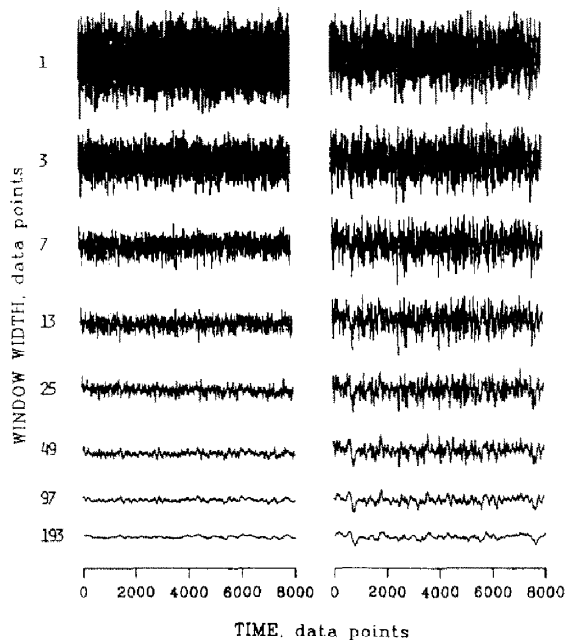

Fig. 7. Traces of AVG-smoothed, single-frequency and multi-frequency simulated Gaussian noise (one set out of five each). Left set: single frequency; right set: multiple frequencies. See text for explanation.

tion assumes initial random noise of only a single frequency —there are no noise components of other speed present to complicate the picture. {The term "frequency" refers here to the imaginary *input* frequency, i.e. the reciprocal of the constant temporal interval between initial data points being introduced into the simulation. It should be recalled, though, that a random input can be considered equivalent to an infinite number of sine waves beating at an infinite number of frequencies (e.g. [20]).}

It is, of course, also possible to introduce random noise at several *different* frequencies, and then smooth the *compounded* initial noise. (For algorithmic convenience, noise of different frequencies is produced here from separate sets of random numbers treated by the AVG filter and multiplied by the square root of the latter's window width to equalize amplitudes. These constituent noise files, and their sum, are thus close to being amplitudinally random.) Although the results of filtering the summed noise are easy to predict, they are still instructive to view. For the right-side traces of Fig. 7, five different noise sources of different temporal input but equal amplitudinal deviation are combined, and the result divided by five. The comparison of the left and right sides of Fig. 7 shows noisy baselines of an obviously *different* character; although the nature of that difference may be hard to put into words.

It is, however, easy to put into numbers: the upper part of Fig. 9 shows the N_{p-p} and RMS curves as derived from five independent replicates of the entire procedure. The procedure simulates —for the left side of the Fig. 9 plot— the response of aboriginal multi-frequency noise to filters of comparable window width; mimicking, for instance, the behaviour of a chromatographic baseline containing random source noise with initial frequencies in, say, the 10–0.3-Hz range, and being filtered with time constants in the 0.1–100-s range.

The results of filtering initial *multi*-frequency noise can be compared with the results of filtering initial *single*-frequency noise (for the latter, see Fig. 8). It is obvious why Fig. 9 displays a flatter section (very roughly of slope 1/4 in the
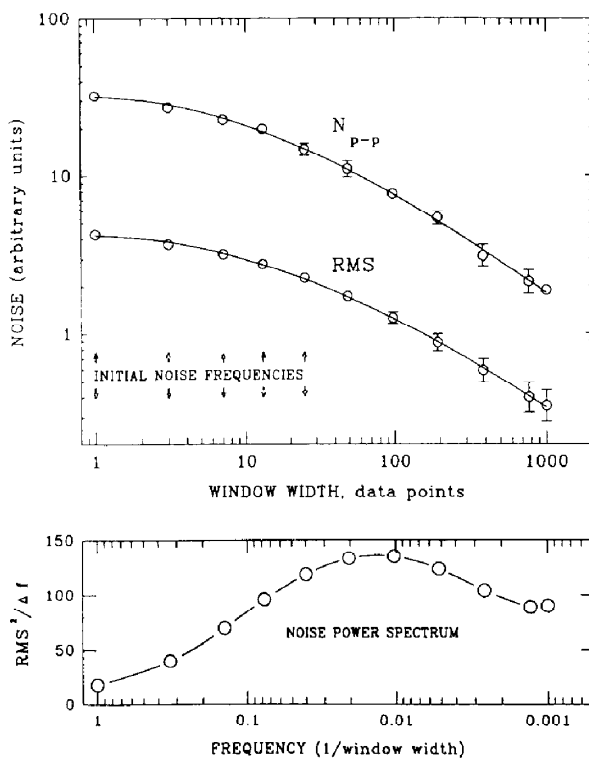

Fig. 9. Measurements on simulated multi-frequency, equal-amplitude noise, smoothed by AVG filter. Upper graph: N_{p-p} ($= N_{all}$) and RMS; lower graph: conventional "noise power spectrum". Data points are averages of five independent sets (one set is shown on the right side of Fig. 7).

region where noise was introduced, as compared to the following, steeper region roughly of slope 1/2). The narrow window widths can reduce only the faster, not the slower noise components. Once the window width exceeds the time constants (the reciprocals of the introduction frequencies) of all five initial noise components, the curve resumes its familiar square-root slope. That, as in Fig. 8, is then merely the wake, i.e. the inherent residual, of the initial perturbations. Regardless of slope, however, the N_{p-p}/RMS ratio keeps *decreasing throughout* the whole time range. This is most important; and in this, single- and multi-frequency noise are alike. What this finding suggests is that the N_{p-p}/RMS ratio will decrease with the extent of filtering regardless of noise speed and composition.

Since the upper graph of Fig. 9 relies on an

unconventional choice of axes to suit the purpose of this study, we repeat for general interest —but refrain from discussing— its RMS result as a conventional "noise power spectrum" in the lower graph. (A similar graph for Fig. 8 would have simply shown the horizontal line considered characteristic of "white" noise [4,20,36]).

3.8. Again: sundry detectors, sundry filters

So far, the experimental curves used only FPD noise. What about FID and ECD noise? Fig. 10 shows these, plus a photomultiplier tube dark current noise —all as taken from the same, conventional electrometer and filtered by the same, common FIR filter. (The "unfiltered" noise levels are arbitrarily included in Fig. 10 at the RC time constant of the electrometer, i.e. at 0.22 s.)

Fig. 10 shows some expected and some unexpected features. The N_{all}/RMS ratios again decrease with the filter time constant as expected. Also as expected, differences show up between different detectors. What seems unexpected, however, is that all (least-squares second-order regression) curves are clearly nonlinear; and that their slopes vary from roughly zero to roughly one. Are the FID and the ECD, as well as the photomultiplier tube dark current, fundamentally different from the FPD that produced the close-to-square-root slope of Fig. 1?

The answer is no —and part of that answer can be given by a cogent experiment that uses the same FPD flame but samples it by two different acquisition systems. Its results are displayed in Fig. 11. The top part of Fig. 11 shows the "regular FPD" noise, i.e. noise that came through the same electrometer (and the same FIR filter) as the three noise records of Fig. 10: both figures are hence of the same bent. It does indeed make sense that the time constant of the electrometer —which is different in nature and
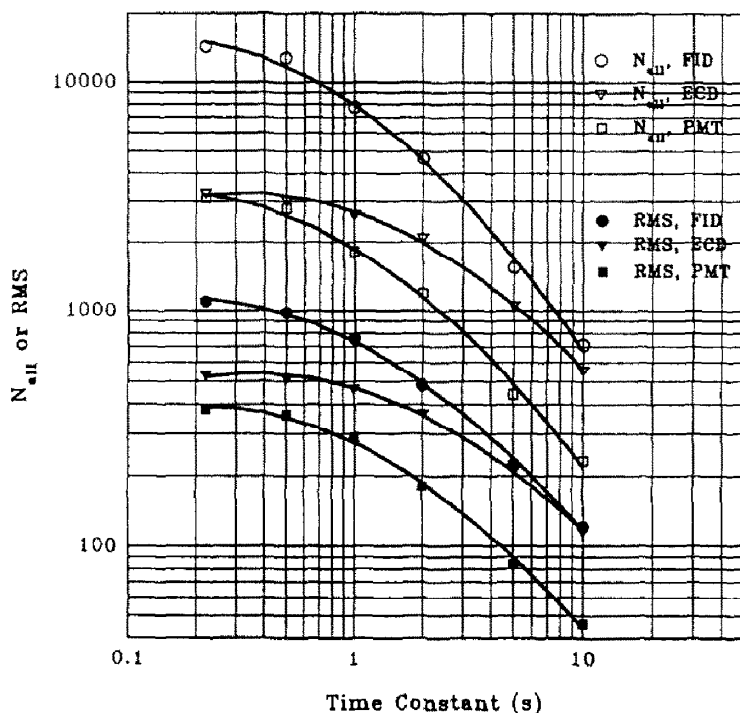

Fig. 10. Measurements on FID, ECD and photomultiplier tube (PMT) noise sources. Electrometer (RC time constant 0.22 s) and FIR filter. Second-order least-squares regression lines.
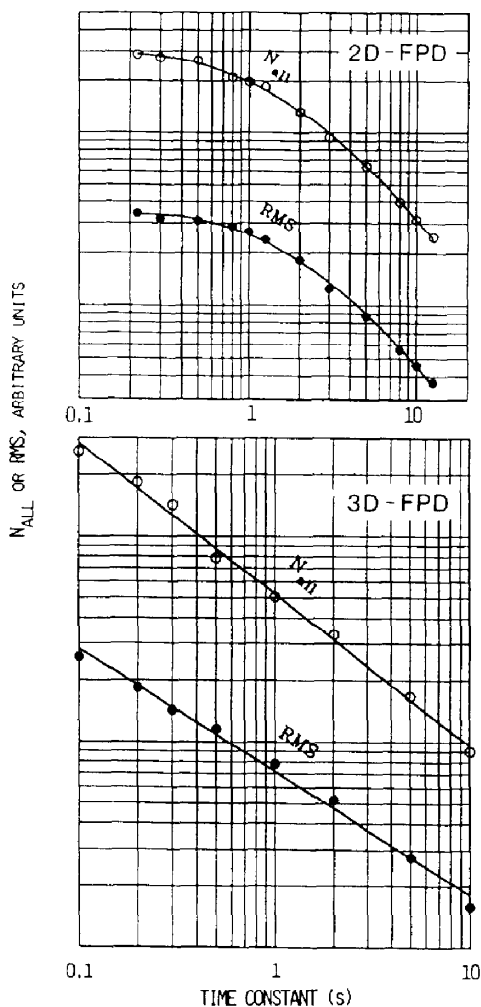
Fig. 11. Measurements on the same FPD noise source via slow and fast acquisition systems. Top: 2D-FPD, otherwise as in Fig. 10; bottom: 3D-FPD [7], first-order least-squares regression lines.

larger in value than the time constant of the fast 3D-FPD acquisition system [7]— should reduce the slope to essentially zero: in that region the noise is already filtered; and as a consequence the expected FIR filter action is largely pre-empted. In contrast, the bottom part of Fig. 11 shows the data for the much faster 3D-FPD system. This system is linear. As expected, the N_{all}/RMS ratio again varies —approximately from 10 to 5— and the (least-squares linear

regression) RMS line shows a slope very close to 0.5.

3.9. General guidelines?

The central question of this study, i.e. the correlation between peak-to-peak and standard-deviation based measurements, can now be addressed for the present noise sources and their conditions. It is obvious that no single or single-series measurement can adequately establish such a correlation for *general* use. Nor can theoretical relationships be confidently employed as long as the distribution of noise has not been experimentally determined. The best that can be done under the circumstances is to estimate its range of behaviour over as many typical cases and conditions as possible.

This has been done in Fig. 12. Ten early experimental series are represented, comprising five types of noise sources, three types of filters, and three types of noise definitions (the fourth one available, σ_{fit}, was excluded: it would have made this particular representation less user-friendly without adding any significant new information). The overall variation of the N_{p-p}/RMS ratio covers the range from about 2 to 10 in this self-explanatory bar graph. The bars extend from the largest to the smallest ratio measured in each experimental set; in general, large ratios are derived from little-filtered, small ratios from much-filtered runs. The left ordinate shows the ratio itself; while the right ordinate shows the multiplication factor thereby implied for converting DL_{spec} at S/RMS = 3 to DL_{chrom} at S/N_{p-p} = 2.

Fig. 12 reinforces earlier conclusions: comparing the peak-to-peak and RMS based measurements of noise is like comparing apples and oranges tumbling out of chromatography's cornucopia. There is no simple and clear connection between the two, and what there is depends to a large extent on conditions. Thus, if the matter is deemed important enough to follow through —that is if *both* types of detection limits *must* be reported— it is up to the analyst to *measure both* under the prevailing laboratory conditions. Obviously, however, that process is time-consuming.
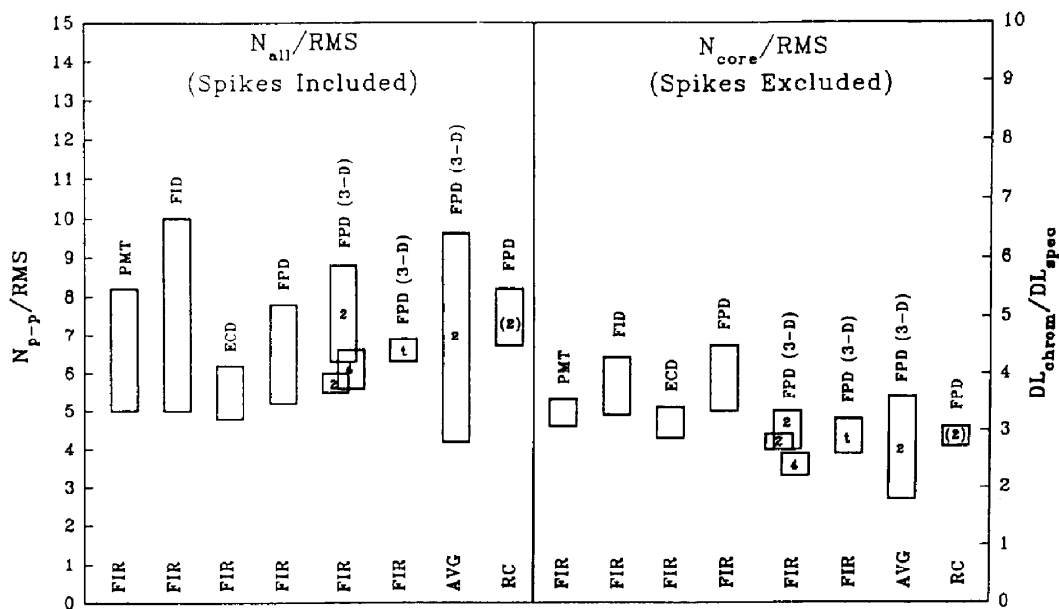
Fig. 12. Comparison of $N_{p\text{-}p}$/RMS and DL_{chrom}/DL_{spec} ranges for different detector and filter combinations. 2, 4 = Segment number in 3D-FPD; (2) = segment number 2, but monitored through stationary wheel via electrometer; t = total of 10 segments in 3D-FPD; PMT = dark current of a Hamamatsu R-374 photomultiplier tube.

Thus there is still some *practical* value in an attempt to narrow conditions and thereby tighten correlations, to the point where a however rough conversion factor may be made to serve less exacting demands. For chromatographic expediency (and only for that) we shall therefore try to come up with a few, very approximate guidelines.

The difference between the "spikes included" N_{all}/RMS and the "spikes excluded" N_{core}/RMS values in Fig. 12 is substantial; as expected it is mainly due to unsmoothed (really: lightly smoothed) noise specimen: their highest values are 10 and 6.8, respectively. With heavy smoothing, the two ratios move closer together (compare also Table 1). Thus the range of values is usually wider in the "spikes *included*" sets. These circumstances would suggest that, for a reasonably repeatable correlation of $N_{p\text{-}p}$ and RMS-based detection limits, the subjective "spikes excluded" measurement might prove the analyst's method of choice if true spikes are present and the smoothing is but light. If spikes are absent and the smoothing is heavy, the analyst may prefer the objective "spikes included" treatment. (The earlier mentioned statistical exclusion of outliers may ameliorate the dilemma this causes for some of the more discriminating software designers.)

On *heavily* smoothed data sets from the three conventional detectors FID, ECD and FPD, the N_{all}/RMS ratio usually falls between 5 and 6, remarkably close to the "$N_{p\text{-}p} = 5$ RMS" spectroscopic rule-of-thumb (e.g. [3,4]). That implies a range of 3.3 to 4 for the DL_{chrom}/DL_{spec} ratio. The N_{core}/RMS ratios are smaller, but not by much. (These numbers depend, of course, on the permissible extent of smoothing, that is to say on the width of the analyte peak. As will be shown later, the longest time constants used for Fig. 12 would have not just smoothed but smothered a really fast chromatogram.)

3.10. Filters and signal/noise ratios: a practical example

The general "guidelines" suggested above for estimating noise, noise ratios and detection-limit

conversion factors do go at least as far as the data of Fig. 12 allow. Therefore, and for the purpose of illustration, we would like to examine the real-life example of a "detection-limit" file. (This is one of the easily characterized, manipulated, and displayed "noise-cum-analyte" files from our 3D-FPD repository. However, similar files from the 2D-FPD, the ECD and the FPD would, mutatis mutandis, have produced similar results.) The *same* data file is treated here with three *different* filters, to the extent reasonable or possible. A small part (5 min out of 12) of the original data file is displayed on the left side of Fig. 13. It calls to mind Ambrose Bierce's definition of noise as "the chief product and
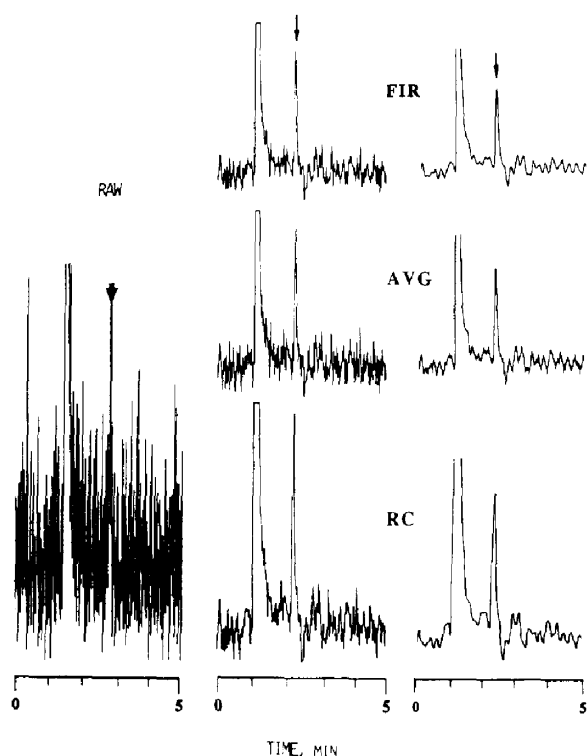

Fig. 13. Five minutes of 3D-FPD noise, with solvent and analyte peak, as smoothed by FIR, AVG and RC filters. Left: raw data file; laser printer; with added arrow marking the analyte peak. Middle: file smoothed to the $S/N_{10\%}$ level by FIR and AVG filter (laser printer) and RC filter (recorder); RC chromatogram adjusted for equal retention. Right: same as middle, but file smoothed to the S/N_{max} level by FIR, and to the strongest setting available by AVG and RC filters. See text for further explanations.

authenticating sign of civilization" (Ref. [37]; substitute "chromatography" for "civilization").

As the noise of the original Fig. 13 data file is being suppressed by the filters, and the analyte peak slowly emerges, the question arises to what level the process can or should be taken. At first thought, this level might be the *maximum* signal/noise ratio (S/N_{max}), at least for straightforward qualitative detection. If, however, the filtered data file is also to be used for quantitation, the argument could be made that the peak height should not be unduly truncated by the smoothing process. Therefore we add a detection-limit assessment at the particular level of filtering that reduces the peak height by an —arbitrary but still generally tolerable— 10% $(S/N_{10\%})$. As it turns out, all three filters are capable of reaching that level. Corresponding parts of the $S/N_{10\%}$ and S/N_{max} chromatograms are displayed in the middle and on the right side of Fig. 13, respectively. Fig. 14 translates these to numbers and plots them in a format conducive to putting forth some simple arguments.

In order to emphasize the controlling role of the analyte peak —whose width defines the extent of smoothing possible or permissible (e.g. [29])— the curves of Fig. 14 are normalized such that the 10% peak-height reduction appears at the same position; and that the three lines are superimposed on one another. This necessitates the use of three formally different abscissae. There is, however, no real contradiction between these three different scales. Time constants of different types of filters cannot be directly compared. Filter action depends on the nature as well as on the sophistication of the particular filter mechanism or algorithm; and the transfer functions of the three filters, operating here on not-quite-Gaussian noise, can at best be roughly estimated. The most glaring difference, i.e. the approximate factor of 1.7 between the time constants of the low-pass RC filter on one hand, and the AVG moving window on the other, is indeed expected [4,20].

All three curves in the top graph —a semilogarithmic plot of peak height reduction vs. filter time constant— appear to be linear. When the top graph is compared with the bottom
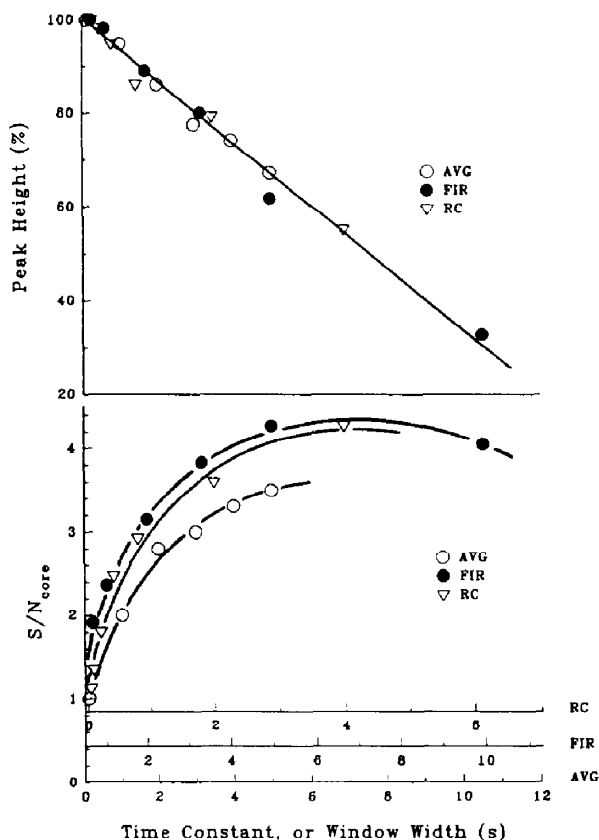
Fig. 14. Corresponding plots of reduction in peak height and S/N vs. nominal time constants of FIR (●), AVG (○) and RC (▽) filters.

graph, it turns out that the S/N increases until the peak height has been reduced by roughly one half! To filter that far may or may not endanger accuracy: how far the process can be driven obviously depends on the particular objectives of analysis and analyst (cf. [29]).

As expected, the fast but unweighted AVG filter performs less well than the slow but weighted FIR filter (running on its maximum of 128 taps). In terms of practical use, however, the difference is decidedly minor. The AVG and RC filters do not overtly reach the S/N_{max} level, but must be close to doing so. The three-pole RC filter is a very simple representative of its kind. Considerably sharper roll-offs can be achieved with units of higher order, say five- or six-pole filters. Again, however, the main advantage of

the higher-order filters may only be that they can work a bit closer to the analyte peak without seriously cropping it —a small and usually negligible advantage if no initial noise components are present in that frequency region.

The reader may indeed be surprised at how little the three disparate filters differ in chromatographic performance. Filters, particularly complex and expensive ones, are designed to cut on and/or cut off within the smallest time-constant increment, i.e. they are expected to offer the sharpest roll-offs. Thus they are often judged by how well they can suppress *sine* waves of one frequency versus another [36]. Yet most of the slow noise seen in this paper appears to be just the square-root carry-over (transform) of fast noise: it represents an unavoidable, *minimum* contribution. Truly fast and random noise, in the Gestalt of a slow-moving transform, just can not be circumvented, subtracted or, for that matter, further suppressed by *any* algorithm. (In contrast, if the initial noise were to contain additional, sizeable amounts of *truly* slow components —components close but not equal to the chromatographic dispersion of the analyte peak— then the *higher*-order filters should, on a *relative* basis, provide larger improvements in the detection limit.)

It may be asked what typical improvement in noise —hence in detection limits— the chromatographer could expect from filtering a particular chromatogram; given that most of the initial noise was fast and random and that the filter did not unduly diminish the analyte peak. The fairly obvious answer is that the noise should be reduced by a factor of approximately $(t_F/t_A)^{1/2}$, where t_F and t_A are the (effective, comparable) time constants of filter and amplifier. As a typical order-of-magnitude example, the chromatographically permissible time constant of an RC filter may be 1 s, and the RC constant of the electrometer circuit that feeds it 0.1 s. The approximate decrease in noise the analyst can then expect from the filter is $10^{1/2}$, i.e. about threefold —and the approximate increase in S/N should be the same (provided the peak height has not been significantly compromised). This does, indeed, agree with our practi-

cal experience, in which we find that filters improve detection limits for conventional detector channels by factors of, typically, three to four.

On the other hand, fast acquisition systems, like that of the 3D-FPD, allow more noise to be transferred. Hence they will also allow more noise to be removed over the now wider frequency range of the smoothing process: such systems will appear to offer larger improvement factors. For instance, the maximum S/N improvement shown in Fig. 14 is close to sixfold. It is similarly obvious that excessively spiky baselines lead to apparently larger improvement factors (for the same time-constant ratio of filtered to unfiltered data), particularly if noise is measured as N_{all}.

The data of Fig. 14 do portray the situation correctly; however, they do not convey the full perceptual impact that the analyst may require for optimal pattern recognition and chromatographic diagnosis, or that the reader may desire for an appreciation of how far the smoothing process can actually be driven. This is one reason why we prefer to report our laboratory's (and assess other laboratories') detection limits in original graphic form, i.e. in the form of analyte peaks surrounded by noise, displayed above the chromatographic time scale (and perhaps supplemented in the caption by the effective filter constant) —rather than in the form of single and possibly equivocal numbers. Also, seeing is believing: the reader may have wondered whether it is really possible to derive relatively clean data —as those of Fig. 14— from a chromatogram as shown on the left side of Fig. 13; and whether the action of the three disparate filters is really that alike.

Accordingly, the results of the three filtering processes are presented first for $S/N_{10\%}$ in the middle, then for S/N_{max} (FIR) or the highest available filter setting (AVG and RC) on the right side of Fig. 13. FIR- and AVG-smoothed traces are reproduced on the laser printer, while the RC-smoothed trace is, of necessity, recorded on a chart and then amplified on a copier to obtain the same retention time scale for chromatographic line-up. (While that procedure does

not change S/N, both peaks and noise appear a bit larger in comparison.)

To our eyes at least, noise at $S/N_{10\%}$ still appears faster than, hence qualitatively different from, the analyte peak. At S/N_{max}, this difference has essentially vanished: noise could now be perceived as a sequence of smaller peaks (particularly if this were a temperature-programmed run). In other words, the analyte peaks are distinguished by both size and width from the former type of noise, by size only from the latter type of noise. Obviously, *two* perceptional dimensions provide more acute discrimination —hence bestow higher confidence— than just one. It is for this reason that, despite the lower S/N, our group actually prefers to use filter settings close to those of $S/N_{10\%}$; even if merely qualitative evaluation is at stake. We realize, however, that such choice depends not only on the analytical objective, but also on the chromatographic experience and perceptual acuity of the individual analyst.

3.11. Adding perspective (some of it in revision)

To add the obvious: The experiments above —for sake of a clearer, preciser look at the subject— have evaluated the S/N of a *single* data file. Other data files will display the same relative behavior, though not the same absolute number. When a single-data-file S/N is changed into a conventional detection limit, the precision implied by, e.g., Fig. 14 may prove delusive. The detection limit must still remain a *one*-significant-digit number; and that it does can be ascertained by comparing different data files or different experimental series. While interesting in their own right, the differences between three types of filters, or between $S/N_{10\%}$ and S/N_{max}, or between N_{all} and N_{core} are —when measured from *one* data file— generally smaller than the corresponding differences between *two* data files treated by the *same* filter and evaluated according to the *same* definition.

In this context, we believe that a protocol for measuring detection limits would be helpful. Yet, we would also consider it presumptuous for us to

suggest one: this not only because we feel less qualified than others to do so, but also because a prematurely suggested protocol might hinder rather than help the advent of eventual consensus. Accordingly, we will be content to pose a few simple questions (sometimes parenthetically accompanied by our own biases) to make a few (im?)pertinent points.

Given its much better precision, is the analyst to choose and use but a *single* data file for determining the detection limit? Or should the analyst go for the best, or the worst, or the average (with or without standard deviation?) of *multiple* data files? (We are accustomed to using a "typical" one —whatever "typical" may mean in this context.) Furthermore, is the detector at its best, typical or worst performance during the measurement? And is the choice of test substances and chromatographic settings designed for general use, for a particular analysis, or for obtaining the lowest possible value of the detection limit? (We usually attempt to follow literature precedents —unless our own choice of standards and circumstances should yield better results.) *It is these choices* that often cause the largest discrepancies among reported DL values. It has been claimed, for instance, that commercial FIDs —most of which are of similar sensitivity— differ by an order of magnitude in their advertised detection limits.

Note that this does not deny noise analysis its proper place in the determination of detection limits —it just cautions that noise characteristics may be overwhelmed by extraneous circumstances of greater variance. Note also that we are concerned here only with *detector* noise —while the consideration of real-life samples must obviously involve not just detection but the *whole* analytical procedure including sampling. But that is, of course, another and far more complex problem.

However flawed, detection limits will continue to remain indispensable tools of the analytical trade. Nevertheless, chromatographers contemplating the use of a published method or the purchase of an advertised detector may well prefer to investigate —before they invest— a claimed "detection limit" with the help of their own standards and in accord with their own definitions.

Acknowledgement

References

[1] J.P. Foley and J.G. Dorsey, *Chromatographia*, 18 (1984) 503.
[2] J.E. Knoll, *J. Chromatogr. Sci.*, 23 (1985) 422.
[3] T.C. O'Haver, in J.D. Winefordner (Editor), *Trace Analysis (Chemical Analysis*, Vol. 46), Wiley, New York, 1976, p. 28.
[4] J.D. Ingle, Jr. and S.R. Crouch, *Spectrochemical Analysis*, Prentice-Hall, Englewood Cliffs, NJ, 1988, mainly around pp. 136–140.
[5] L.A. Currie, in L.A. Currie (Editor), *Detection in Analytical Chemistry (ACS Symposium Series*, No. 361), American Chemical Society, Washington, DC, 1988, p. 33.
[6] X.-Y. Sun, B. Millier and W.A. Aue, *Can. J. Chem.*, 70 (1992) 1129.
[7] B. Millier, X.-Y. Sun and W.A. Aue, *J. Chromatogr. A*, 675 (1994) 155.
[8] S.D. Brown, in S.J. Haswell (Editor), *Practical Guide to Chemometrics*, Marcel Dekker, New York, 1992, p. 239.
[9] H.G. Hecht, *Mathematics in Chemistry*, Prentice-Hall, Englewoood Cliffs, NJ, 1990.
[10] N. Dyson, *Chromatographic Integration Methods (RSC Chromatography Monographs)*, Royal Society of Chemistry, Cambridge, 1990.
[11] R.G. Brereton, *Chemometrics*, Ellis Horwood, New York, 1990.
[12] D.L. Massart, B.G.M. Vandeginste, S.N. Deming, Y. Michotte and L. Kaufman, *Chemometrics*, Elsevier, Amsterdam, 1988.
[13] J.D. Ingle, Jr. and S.R. Crouch, *Spectrochemical Analysis*, Prentice-Hall, Englewood Cliffs, NJ, 1988, pp. 172–176.
[14] G.L. Long and J.D. Winefordner, *Anal. Chem.*, 55 (1983) 713A.
[15] Analytical Methods Committee, *Analyst*, 112 (1987) 199.
[16] P.W.J.M. Boumans, *Spectrochim. Acta*, 46B (1991) 431, 917.
[17] L.A. Currie (Editor), *Detection in Analytical Chemistry (ACS Symposium Series*, No. 361), American Chemical Society, Washington, DC, 1988.
[18] R.W. Hamming, *Digital Filters*, Prentice Hall, Englewood Cliffs, NY, 2nd ed., 1983.

[19] W.A. Aue, B. Millier and X.-Y. Sun, *Can. J. Chem.*, 70 (1992) 1143.

[20] C.T.J. Alkemade, W. Snelleman, G.D. Boutilier, B.D. Pollard, J.D. Winefordner, T.L. Chester and N. Omenetto, *Spectrochim. Acta*, 33B (1978) 383.

[21] E.P. Grimsrud, in H.H. Hill, Jr. and D.G. McMinn (Editors), *Detectors for Capillary Chromatography (Chemical Analysis*, Vol. 121), Wiley-Interscience, New York, 1992, Ch. 5.

[22] A. Zlatkis and C.F. Poole (Editors), *Electron Capture (Journal of Chromatography Library*, Vol. 20), Elsevier, Amsterdam, 1981.

[23] J. Connor, *J. Chromatogr.*, 200 (1980) 15.

[24] W.A. Aue and S. Kapila, *J. Chromatogr.*, 188 (1980) 1.

[25] W.A. Aue, K.W.M. Siu, D. Beauchemin and S.S. Berman, *J. Chromatogr.*, 500 (1990) 95.

[26] D.G. McMinn and H.H. Hill, Jr., in H.H. Hill, Jr. and D.G. McMinn (Editors), *Detectors for Capillary Chromatography (Chemical Analysis*, Vol. 121), Wiley-Interscience, New York, 1992, Ch. 2.

[27] S.J. Haswell (Editor), *Practical Guide to Chemometrics*, Marcel Dekker, New York, 1992.

[28] H.C. Smit and H.L. Walg, *Chromatographia*, 8 (1975) 311.

[29] C.G. Enke and T.A. Nieman, *Anal. Chem.*, 48 (1976) 705A.

[30] *Nomenclature for Chromatography (IUPAC Recommendation 1993); Pure Appl. Chem.*, 65 (1993) 819 (p. 851).

[31] *ASTM E 685-79*, American Society for Testing and Materials, Philadelphia, PA, 1st ed., 1981; as shown by N. Dyson, *Chromatographic Integration Methods (RSC Chromatography Monographs)*, Royal Society of Chemistry, Cambridge, 1990.

[32] C. Chatfield, *The Analysis of Time Series*, Chapman & Hall, London, 4th ed., 1989.

[33] P. Gray, *Psychology*, Worth Publishers, New York, 1991, Ch. 9.

[34] K.W.M. Siu and W.A. Aue, *Can. J. Chem.*, 65 (1987) 1012.

[35] A.W. McMahon and W.A. Aue, *Mikrochim. Acta*, II (1987) 91.

[36] K.W. Busch and M.A. Busch, *Multielement Detection Systems for Spectrochemical Analysis*, Wiley, New York, 1990, e.g. pp. 364–377.

[37] A. Bierce, *The Devil's Dictionary*, Sagamore Press, New York, 1957; as cited by W.R. Bennett, *Electrical Noise*, McGraw-Hill, New York, 1960.